Journal of Materials Research and Technology 42 (2026) 4311–4323

Contents lists available at ScienceDirect

Journal of Materials Research and Technology

journal homepage: www.elsevier.com/locate/jmrt

# Property relationships study of sugar palm fiber-reinforced recycled HDPE bottle-cap composites

Rahmat Doni Widodo [a,*], Muhammad Irfan Nuryanta [a], Prima Astuti Handayani [b], Rizky Ichwan [b], Edi Syams Zainudin [c], Muhammad Akhsin Muflikhun [d]

[a] Department of Mechanical Engineering, Universitas Negeri Semarang, Semarang, Indonesia
[b] Department of Chemical Engineering, Faculty of Engineering, Universitas Negeri Semarang, Semarang, 50229, Indonesia
[c] Advanced Engineering Materials and Composite Research Centre (AEMC), Department of Mechanical and Manufacturing Engineering, Universiti Putra Malaysia, 43400, UPM Serdang, Selangor, Malaysia
[d] Department of Mechanical and Industrial Engineering, Faculty of Engineering, Universitas Gadjah Mada, Jl. Grafika No. 2, Yogyakarta, 55281, Indonesia

ARTICLE INFO

*Keywords:*
rHDPE
Bottle cap
Sugar palm fiber
Natural fiber
Composite
Mechanical properties

ABSTRACT

Post-consumer high-density polyethylene (rHDPE) bottle caps represent an abundant waste stream with potential for use in semi-structural composite applications, although their mechanical performance remains limited. This study investigated the feasibility of reinforcing recycled HDPE bottle-cap composites with alkali-treated sugar palm (*Arenga pinnata*) fiber at loadings of 0, 10, 15, and 20 wt%. The composites were fabricated by manual melt mixing followed by hot pressing and evaluated in terms of density, 24 h water absorption, tensile, flexural (dry and water-conditioned), and Charpy impact properties, together with FTIR, DSC, and SEM characterization. The density increased from 0.949 to 0.983 g/cm$^3$ with increasing fiber content, while the tensile strength improved markedly from 11.52 MPa for neat rHDPE to 20.92 MPa at 20 wt% fiber. Water absorption increased from 0.00% to 1.16% as fiber loading increased. The impact strength reached its maximum at 15 wt% (15.75 kJ/m$^2$) before decreasing at 20 wt%, indicating an optimum fiber content for toughness. Under water-conditioned flexural testing, composites with 10–15 wt% fiber exhibited better wet/dry strength retention (63.25–63.35%) than neat rHDPE (52.16%), whereas 20 wt% fiber resulted in reduced retention. FTIR confirmed the presence of lignocellulosic constituents in the composite, while DSC showed only minor variation in melting temperature, suggesting that the mechanical response was governed mainly by reinforcement efficiency and microstructural features. Overall, 10–15 wt% alkali-treated sugar palm fiber provided the best balance of impact resistance and wet-strength retention, demonstrating a practical route for upgrading recycled HDPE bottle caps into lightweight engineering composites.

## 1. Introduction

Post-consumer plastic waste continues to accumulate at an alarming rate, with high-density polyethylene (HDPE), particularly from packaging components such as bottle caps, contributing significantly to this stream. Converting HDPE waste into value-added materials has therefore emerged as an important strategy in addressing sustainability challenges [1–3]. In this context, recycled HDPE is widely considered as a composite matrix due to its favorable chemical resistance and ease of processing. Nevertheless, its mechanical performance is often inferior to that of virgin polymers, primarily due to prior thermomechanical degradation, contamination, and chain scission during repeated processing cycles [4]. This limitation has constrained its broader application in engineering and semi-structural components [5–7], highlighting the need for effective reinforcement strategies that do not compromise environmental benefits.

Natural fibers have attracted considerable attention as reinforcing agents for recycled thermoplastics, offering advantages such as low density, renewability, and cost efficiency [4,8–10]. Several studies have demonstrated that the incorporation of lignocellulosic fibers can improve stiffness and specific mechanical properties of polymer composites [9,11]. However, two key challenges remain. First, the inherent polarity mismatch between hydrophilic natural fibers and hydrophobic polyolefin matrices often leads to weak interfacial adhesion [12].

* Corresponding author.
*E-mail address:* rahmat.doni@mail.unnes.ac.id (R.D. Widodo).

https://doi.org/10.1016/j.jmrt.2026.04.117
Received 27 January 2026; Received in revised form 9 April 2026; Accepted 13 April 2026
Available online 15 April 2026

Second, the tendency of natural fibers to absorb moisture can further deteriorate the fiber–matrix interface and accelerate mechanical degradation over time [13]. These issues are often exacerbated in recycled polymer systems, where material heterogeneity can intensify interfacial defects [14].

Sugar palm fiber (*Arenga pinnata*) is an abundant natural resource in tropical regions and exhibits promising characteristics, including good durability and resistance to biological degradation [15,16]. Despite these advantages, its application as a reinforcement in thermoplastic composites has not been extensively explored. Like other lignocellulosic fibers, the presence of hydroxyl-rich functional groups in sugar palm fiber limits its compatibility with hydrophobic matrices such as HDPE, which can result in poor stress transfer and premature failure [17]. In the present study, recycled HDPE and sugar palm fiber are combined based on a set of complementary considerations. From an economic perspective, both materials are low-cost and readily available, with HDPE sourced from post-consumer bottle cap waste and sugar palm fiber obtained as an agricultural by-product in tropical regions [10,15]. From a materials standpoint, while recycled HDPE retains desirable properties such as chemical resistance and processability, its reduced mechanical strength necessitates reinforcement. Sugar palm fiber offers a suitable solution due to its low density, inherent durability, and relatively strong resistance to biological attack compared with many other lignocellulosic fibers [15,16]. From an application perspective, integrating recycled polymers with renewable natural fibers is consistent with circular economy principles and provides a sustainable pathway for developing low-density, value-added composites for semi-structural applications [5,8]. Accordingly, surface modification is generally required to enhance interfacial interaction between the fiber and matrix, thereby improving load transfer efficiency and overall composite performance [3,18].

Among the various surface modification techniques, alkali treatment using sodium hydroxide (NaOH) is one of the most widely adopted methods for natural fibers due to its simplicity and effectiveness. This treatment facilitates the removal of surface impurities and the partial dissolution of non-cellulosic constituents, including waxes, hemicelluloses, and lignin [13,19,20], while simultaneously increasing surface roughness and exposing cellulose microfibrils [21]. Such modifications are generally associated with improved mechanical interlocking and enhanced interfacial adhesion, which can contribute to better overall composite performance [22]. However, the effectiveness of alkali treatment is highly dependent on several factors, including fiber type [23], treatment parameters, and fiber loading. Moreover, the reinforcing behavior of alkali-treated short sugar palm fibers in recycled HDPE matrix particularly those derived from post-consumer bottle caps has not yet been fully established [24].

In recent years, the development of sustainable materials has increasingly emphasized natural fiber reinforced polymer composites, driven by their low density and favorable environmental profile [8,10,25]. Although research on recycled polyolefin-based composites reinforced with natural fibers is growing, systematic investigations focusing specifically on recycled HDPE bottle-cap composites reinforced with alkali-treated short sugar palm fibers remain limited. Comprehensive correlations linking mechanical properties, moisture absorption, density, thermal behavior, chemical characteristics, and fracture morphology are still lacking. Furthermore, evaluating mechanical performance under both dry and wet conditions is crucial for assessing application-relevant behavior, especially considering the inherent moisture sensitivity of lignocellulosic fiber composites [15,26,27].

To further emphasize the novelty of this work, Table 1 summarizes selected recent studies on HDPE-based natural fiber composites. While prior studies have predominantly focused on virgin polymers or broadly defined recycled plastics, limited attention has been given to the upcycling of post-consumer rHDPE bottle caps using relatively simple and low-shear processing routes. In addition, moisture-induced degradation particularly through mechanical testing under wet conditions remains underreported in sugar palm fiber reinforced composite systems.

Accordingly, this study aims to establish the structure-property relationships of recycled high-density polyethylene bottle-cap composites reinforced with alkali-treated sugar palm fibers and to determine a practical fiber-loading range for tailoring their mechanical performance and moisture-related behavior. The amount of fiber used varied from 0 to 20 wt%, with the target composites evaluated for density, water absorption and tensile and flexural properties in dry and water-conditioned states, impact resistance and hardness. In addition, complementary analyses were carried out using FTIR to assess chemical structure, DSC to investigate thermal behavior, and SEM to examine fracture morphology. The integration of these multiscale characterizations provides greater insight into the effects of fiber loading and moisture exposure on composite performance while demonstrating a viable, sustainable path for transforming recycled HDPE bottle caps into value-added engineering materials.

## 2. Materials and methods

### 2.1. Materials

Post-consumer HDPE bottle caps (*Le Minerale*) were collected from municipal waste streams in Semarang, Indonesia (Fig. 1a). The caps were manually sorted to remove non-HDPE materials, then washed

**Table 1**
Summary of similar works on HDPE/natural fiber composites and identified research gaps.

| Reference | Matrix + Reinforcement | Methodology | Key Findings | Identified Research Gap |
|---|---|---|---|---|
| [1] | Virgin HDPE + Palm Kernel Shell Particles | Melt compounding and compression | Investigated the mechanical property enhancement using agricultural solid waste. | Utilizes virgin HDPE as the matrix; does not address the upcycling of post-consumer plastic waste streams. |
| [28] | Recycled PET (bottle) + recycled HDPE (bottle cap) | Shredding, cleaning, characterization, and direct fused granular/fused particle 3D printing with parameter optimization | Direct printing from mixed PET/HDPE waste was technically feasible and might lower manufacturing costs, but warping and delamination remained significant problems. | Focused on mixed-waste 3D printing rather than natural fiber-reinforced composites; did not address wet-condition mechanical retention or structure–property relationships in recycled HDPE bottle-cap composites |
| [29] | Recycled HDPE + Natural Fibers + Waste Tire Rubber | Injection vs. Compression Molding | Compared the mechanical performance differences based on complex molding techniques. | Relying on complex hybridization and processing methods, moisture sensitivity and wet-condition retention were not the primary focus. |
| [30] | Bottle-cap blend (PE/PP) + banana pseudostem and rachis fibers | Gelimat mixing, injection molding, blending, alkali fiber treatment, and cost, mechanical, and thermal analysis | A bottle-cap blend may replace HDPE, and composites with ≥30 wt% fiber exhibited enhanced mechanical characteristics and superior cost competitiveness. | Utilized blended PE/PP bottle caps instead of recycled HDPE composites; concentrated on increased loading of banana fibers and did not assess water absorption, wet-condition flexural retention, or structure–property correlations using FTIR/SEM analysis of recycled HDPE composites. |

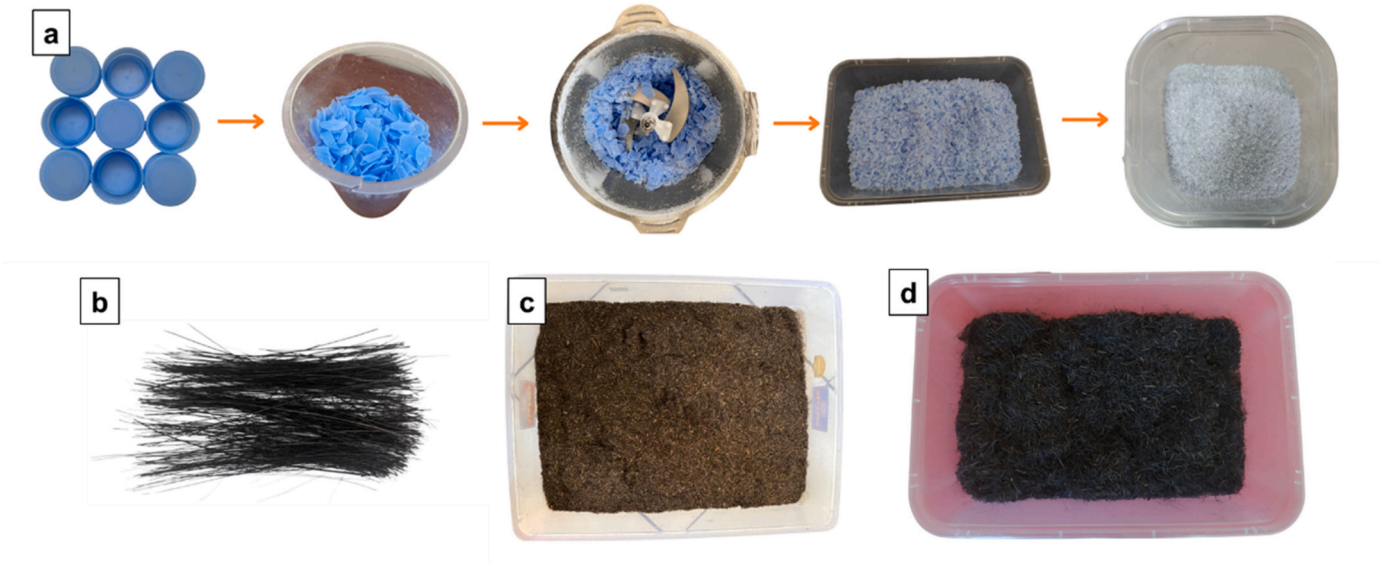


**Fig. 1.** Raw materials and preprocessing stages used for the fabrication of sugar palm fiber-reinforced recycled high-density polyethylene bottle-cap composites: (a) post-consumer bottle caps and their conversion into recycled polymer flakes through cutting and grinding, (b) sugar palm fibers, (c) dried fibers before alkali treatment, and (d) dried fibers after alkali treatment.

using a detergent solution, followed by rinsing with tap water and subsequently with distilled water. The cleaned caps were oven-dried at 60 °C for 25 min, following previously reported conditions for recycled HDPE feedstock preparation. After drying, the caps were cut into smaller pieces using a shredder to produce granules or flakes with irregular geometry. The processed material was then stored in sealed containers prior to further processing.

Sugar palm fibers (*Arenga pinnata*) were obtained from a local supplier in Semarang, Indonesia (Fig. 1b). The fibers were cleaned to remove dust and surface contaminants, thoroughly rinsed, and oven-dried at 60 °C for 1 h. After drying, the fibers were cut into short segments with an average length of approximately 3 mm prior to alkali treatment and subsequent use in composite fabrication.

## 2.2. Methods

### 2.2.1. Alkali treatment of sugar palm fibers

Alkali treatment was performed to enhance fiber–matrix compatibility by removing surface impurities and partially dissolving non-cellulosic constituents [30]. Cleaned and dried sugar palm fibers were immersed in a 5 wt% NaOH aqueous solution, prepared using distilled water, at room temperature for 6 h under mild stirring conditions [31]. The use of ambient temperature was selected based on previous studies [20,31], which indicate that treatment under such conditions effectively removes impurities and non-cellulosic components while avoiding thermal degradation of cellulose microfibrils that may occur at elevated temperatures. A fiber-to-solution ratio of 1:25 (w/v) was maintained to ensure uniform and complete immersion throughout the treatment process [5]. After treatment, the fibers were removed from the solution and rinsed three times with distilled water to eliminate residual NaOH [32]. The rinsed fibers were then drained (Fig. 1c and d) at room temperature for 24 h, followed by oven drying at 60 °C for 3 h to remove any remaining moisture [23]. The treated fibers were subsequently stored in sealed containers prior to composite fabrication [15].

Although direct chemical characterization techniques, such as FTIR or XRD, were not performed on the treated fibers in the present study, the selected alkali treatment parameters, including NaOH concentration and soaking duration, were carefully based on established protocols. As extensively reported in previous studies [17,20,33], such alkaline treatment has been shown to effectively disrupt hydrogen bonding, remove amorphous components such as hemicellulose and lignin, and increase the crystallinity index of cellulose. These structural modifications are known to enhance fiber surface characteristics, thereby contributing to improved mechanical interlocking within the composite matrix.

### 2.2.2. Composite formulation and fabrication

The composites were fabricated at four fiber loadings of 0, 10, 15, and 20 wt%, and the corresponding formulation codes and nominal compositions are summarized in Table 2. Prior to fabrication, the rHDPE flakes were oven-dried at 60 °C for 25 min, while the alkali-treated fibers were dried according to the procedure described in Section 2.2.1, involving 24 h of draining followed by oven drying at 60 °C for 3 h. This pre-drying step was implemented to minimize moisture-induced void formation during processing.

The fiber loadings selected (0, 10, 15 and 20 wt%) are not derived from a rigorous Design of Experiments approach but rather chosen in the scope of ranges reported in previous short natural fiber-reinforced thermoplastic composite studies [34,35]. This range was found appropriate for capturing the unreinforced to moderately reinforced state while avoiding higher fiber contents that risk poor dispersion, incomplete matrix wetting and void formation in a batch generally associated with manual premixing/hot-pressing conditions.

For each formulation, the required masses of rHDPE and short fibers were weighed according to the target mass fractions and premixed manual until a visual uniform fiber distribution in the rHDPE feedstock was achieved. Fiber content was defined on a weight basis relative to the total composite mass. The premix was preheated in an oven at 180 °C for 30 min to soften the rHDPE and facilitate consolidation. After 15 min, the blend was removed and manual kneaded with a spatula for 2 min, then returned to the oven for an additional 15 min until the matrix became sufficient softened for molding as shown in Fig. 2. This

**Table 2**
Formulation codes and nominal compositions of recycled high-density polyethylene/sugar palm fiber composites (0–20 wt% fiber).

| Code | Sugar palm fiber content (wt%) | rHDPE (wt%) |
|---|---|---|
| rHDPE–Sugar palm 0 | 0 | 100 |
| rHDPE–Sugar palm 10 | 10 | 90 |
| rHDPE–Sugar palm 15 | 15 | 85 |
| rHDPE–Sugar palm 20 | 20 | 80 |

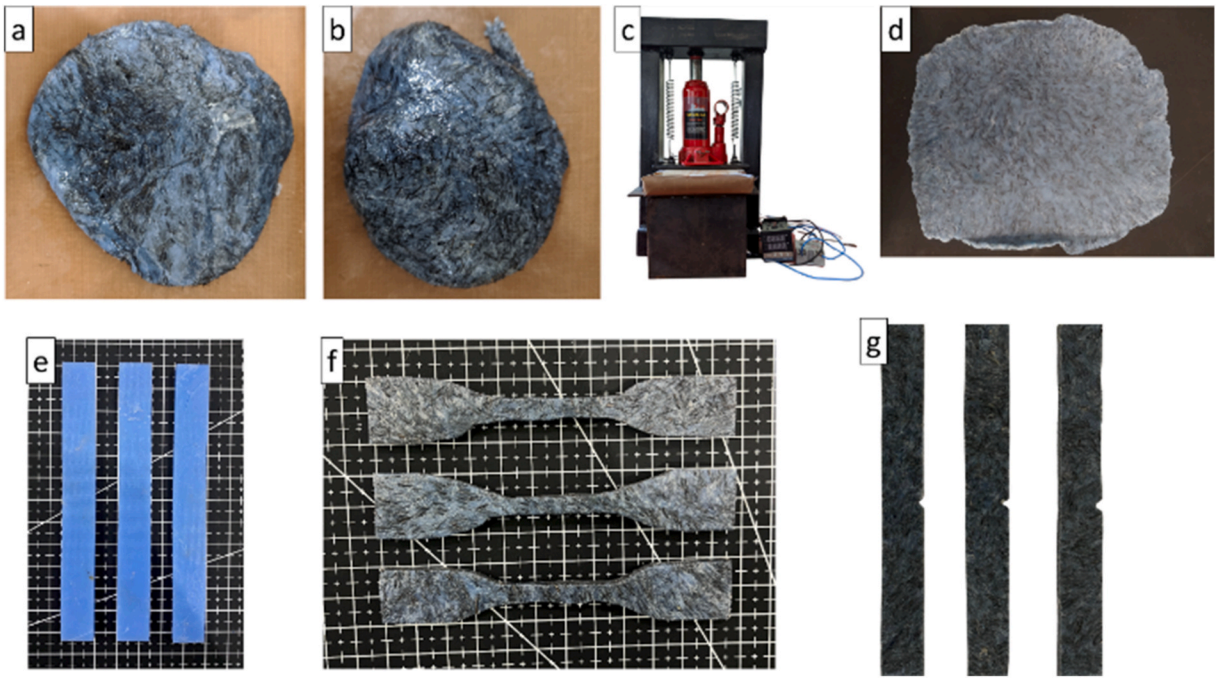


**Fig. 2.** Composite fabrication and specimen preparation: (a) first kneading after the first 15 min of oven preheating, (b) second kneading after the second 15 min, (c) manual hot-press setup used (d) hot-pressed composite plate, (e) flexural specimens, (f) tensile specimens, and (g) Charpy impact specimens.

intermittent kneading step was employed to improve fiber dispersion while limiting continuous thermal exposure.

The softened material was transferred into a preheated steel mold and consolidated by compression molding (hot pressing) at 180 °C for approximate 10 min immediate after preheating [36]. Composite plates were produced with a nominal thickness of 4 mm and cooled to room temperature under pressure to reduce warpage and internal void formation [37]. Standard specimens for tensile, flexural (dry and water-conditioned), impact, and hardness testing were prepared from the molded plates according to the relevant standards. The applicable standards and specimen dimensions used in this study are provided in Table 3.

### 2.2.3. Density measurement

The density of the composite was measured according to ASTM D792 [42] using the Archimedes method with distilled water as the immersion medium at 23 ± 2 °C. Loads were applied when necessary to ensure complete immersion of specimens. At least five specimens were tested for each formulation, and the results were reported as mean ± standard deviation.

**Table 3**
Testing standards and specimen dimensions.

| Test type | Standard | Dimensions (mm) | Number of specimens per formulation (n) | Reference |
|---|---|---|---|---|
| Tensile | ASTM D638 (Type IV) | dog-bone (dimensions per standard), t = 3.5 mm | 3 | [38] |
| Flexural (dry) | ASTM D790 | 122 × 13.2 × 3.5 | 3 | [39] |
| Flexural (wet) | ASTM D790 | 122 × 13.2 × 3.5 | 3 | [39] |
| Impact | ASTM D6110 | Charpy (notch geometry per standard), t = 3.5 mm | 3 | [40] |
| Hardness | ASTM D2240 | 62.5 x 13 x 3.5 | 3 | [41] |

### 2.2.4. Water absorption

Water absorption was evaluated using a simple procedure adapted from ASTM D570 [43] to support the assessment of flexibility under wet conditions. Specimens were dried at 60 °C to constant mass, cooled to room temperature in a closed container to minimize moisture absorption, and weighed using an analytical balance with a resolution of 0.001 g. The samples were then immersed in distilled water at 23 ± 2 °C for 24 h. The specimens were removed after immersion, the surface water was gently wiped off consistently, and their mass was recorded immediately using the same balance. Water absorption was determined from the relative increase in mass compared to the initial dry mass.

### 2.2.5. Tensile testing

Tensile testing was performed using a universal testing machine (UTM) in accordance with ASTM D638. Type IV dog-bone specimens were prepared from the molded composite plates and conditioned at room temperature prior to testing. The tests were conducted at a constant crosshead speed of 2 mm/min. Tensile strength was determined from the maximum stress recorded during testing and the stress–strain response was obtained direct from the load–displacement data [17].

### 2.2.6. Flexural testing under dry and wet conditions

Three-point bending tests were conducted in accordance with ASTM D790. Rectangular specimens with dimensions of approximately 120 mm × 13 mm × 3.5 mm (length × width × thickness) were prepared from the molded plates. The support span was set to 16 times the specimen thickness and the tests were performed at a crosshead speed determined according to the ASTM D790 standard. Flexural strength and flexural modulus were obtained from the load–deflection curves.

For wet-condition flexural testing, specimens were immersed in distilled water at 23 ± 2 °C for 24 h. After immersion, samples were removed, surface water was gently wiped, and the flexural test was performed immediate under the same testing configuration [12].

#### 2.2.7. Impact testing

Impact resistance was measured using the Charpy impact test in accordance with ASTM D6110, employing notched specimens with a notch geometry conforming to the standard (including the specified notch radius). Impact strength was calculated from the absorbed impact energy and reported in kJ/m$^2$.

#### 2.2.8. Hardness testing

Hardness was measured using a Shore D durometer in accordance with ASTM D2240. Indentations were taken at multiple locations on each specimen with adequate spacing to avoid interaction effects, and the average Shore D value was reported for each formulation.

#### 2.2.9. Differential scanning calorimetry (DSC)

Thermal melting behavior of neat rHDPE and rHDPE/sugar palm fiber composites was examined using differential scanning calorimetry (DSC) under a nitrogen atmosphere. To evaluate the melting transition of the rHDPE matrix, the heating scan in the temperature range of 25–200 °C was used for analysis at a heating rate of 10 °C/min. Sample masses were 5.80 mg (rHDPE), 6.40 mg (10 wt%), 5.60 mg (15 wt%), and 5.50 mg (20 wt%). The melting peak temperature (Tm) was determined from the maximum of the melting endotherm. The melting enthalpy is reported as an apparent melting enthalpy (ΔHm,app) obtained by integrating the melting endotherm over the melting region using a consistent baseline approach for all samples, and is presented for comparative purposes across formulations.

#### 2.2.10. Fourier transform infrared spectroscopy (FTIR)

FTIR spectroscopy was carried out to examine the effect of sugar palm fiber loading on the chemical features of the rHDPE composites. Spectra were acquired in the mid-infrared region using an FTIR spectrometer under the instrument default acquisition settings. The FTIR data were recorded as percent transmittance (%T) versus wavenumber (cm$^{-1}$). Spectra of neat rHDPE (0% fiber) and composites containing sugar palm fibers at 10, 15, and 20 wt% were compared to identify changes in characteristic absorption bands associated with the presence and increasing content of lignocellulosic fibers in the rHDPE matrix.

#### 2.2.11. Scanning electron microscopy (SEM)

Fracture surfaces of the tested specimens were examined using scanning electron microscopy (SEM) to provide morphological information related to fracture behavior and composite microstructure. Fragments were taken from the fracture region of tensile and flexural specimens. For specimens previous exposed to water (wet-condition flexural test), the fracture pieces were dried at 60 °C to remove residual moisture prior to observation. The samples were mounted on aluminum stubs using conductive carbon tape and sputter-coated with a 5 μm gold layer to minimize charging during imaging. The SEM micrographs were used for qualitative assessment of features such as fiber distribution, matrix tearing, indications of fiber pull-out or interfacial debonding, and the presence of voids or defects.

## 3. Results and discussion

### 3.1. Density of rHDPE/Sugar palm fiber composites

The density of neat rHDPE and rHDPE composites reinforced with alkali-treated short sugar palm fibers is presented in Fig. 3a. A gradual increase in density was observed with increasing fiber loading. Neat rHDPE (0 wt% fiber) exhibited a density of 0.94936 ± 0.01008 g/cm$^3$, while the composites showed densities of 0.96774 ± 0.00974 g/cm$^3$ (10 wt%), 0.98212 ± 0.00483 g/cm$^3$ (15 wt%), and 0.98324 ± 0.00644 g/cm$^3$ (20 wt%). Overall, the density increased by 3.58% from 0 to 20 wt% fiber. This trend is consistent with the replacement of part of the polymer phase by a lignocellulosic reinforcement that typically has a higher intrinsic density than HDPE and may also influence consolidation during hot pressing.

The scatter of density values also varied with fiber content. The standard deviation decreased at 15 wt% compared with 0 and 10 wt%, indicating more consistent specimen-to-specimen density at this loading, whereas the 20 wt% composite showed slightly higher variability than the 15 wt% composite. Because the composites were prepared through manual premixing followed by hot pressing, minor variations in fiber dispersion and the presence of localized voids cannot be fully ruled out. Accordingly, the density results should be interpreted in conjunction with moisture-related behavior as well as fracture and morphological observations [9]. Nevertheless, the observed monotonic increase in density suggests effective incorporation of sugar palm fibers into the rHDPE matrix, providing a sound physical basis for subsequent comparisons of mechanical properties across the different formulations.

### 3.2. Water absorption after 24 h immersion

After 24 h of water immersion, neat rHDPE (0 wt% fiber) exhibited negligible water absorption (0.000 ± 0.000%), whereas all fiber-reinforced composites showed measurable moisture uptake of 0.397 ± 0.066% (10 wt%), 1.053 ± 0.132% (15 wt%), and 1.164 ± 0.085% (20 wt%). The introduction of 10 wt% sugar palm fiber resulted in an increase in water absorption to 0.397%. A further increase in fiber content from 10 to 15 wt% led to a substantial rise of 0.656 percentage points (from 0.397% to 1.053%), corresponding to a 165% increase relative to the 10 wt% composite. In contrast, increasing the fiber loading from 15 to 20 wt% produced only a modest increment of 0.111 percentage points (from 1.053% to 1.164%), equivalent to a 10.5% increase relative to the 15 wt% composite. This trend suggests that, under the 24 h immersion condition applied in this study, the sensitivity of

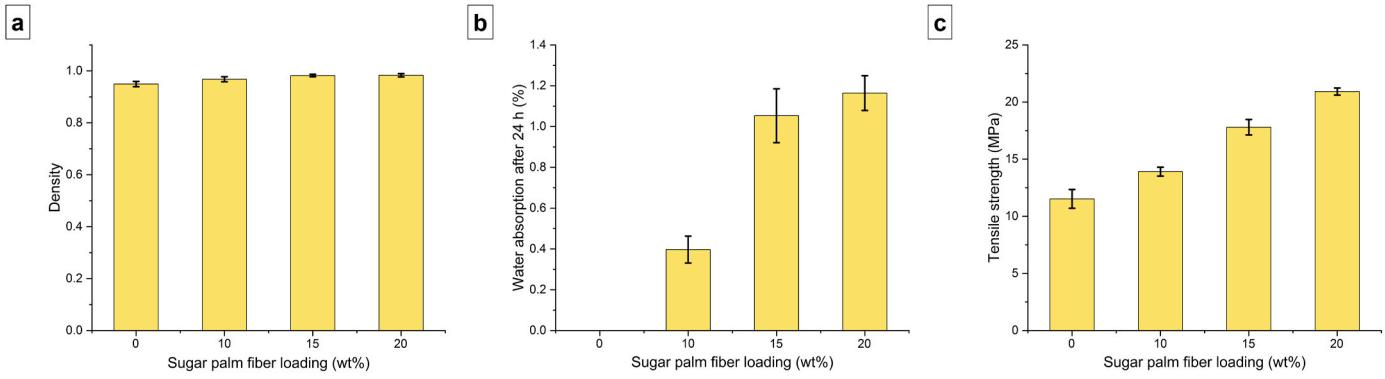


**Fig. 3.** Physical and tensile properties of sugar palm fiber-reinforced recycled high-density polyethylene bottle-cap composites at different fiber loadings: (a) density, (b) water absorption after 24 h immersion, and (c) tensile strength.

water absorption to increasing fiber content diminishes at higher loadings. The corresponding water absorption behavior is presented in Fig. 3b.

The measurement scatter remained relatively small compared to the mean values, indicating good consistency across the triplicate tests. The coefficients of variation were 16.6% (10 wt%), 12.5% (15 wt%), and 7.3% (20 wt%), suggesting acceptable repeatability. The reduced relative variability at higher fiber loadings is consistent with the larger absolute mass changes observed, which improve measurement sensitivity when using a balance with 0.001 g resolution.

From a structure–property perspective, the pronounced increase in water absorption between 10 and 15 wt% indicates that moisture uptake becomes increasingly governed by the higher density of hydrophilic fiber sites and expanded fiber–matrix interfacial regions once the fiber content exceeds 10 wt%. In addition to the intrinsic hygroscopicity of lignocellulosic fibers, increasing fiber loading also raises the likelihood of interfacial micro gaps and diffusion pathways, particularly in composites fabricated through manual premixing and hot pressing. These features can facilitate water ingress into the composite structure [44–46]. The comparatively smaller increase observed between 15 and 20 wt% suggests that, within the 24 h immersion period, a substantial portion of accessible hydrophilic sites and diffusion pathways may already be active, resulting in a diminishing incremental effect with further fiber addition. This behavior is fundamentally linked to the hydrophilic nature of lignocellulosic materials. As highlighted in recent reviews [44,46], the abundance of hydroxyl (–OH) groups in cellulose and hemicellulose promotes hydrogen bonding with water molecules, making increased moisture uptake unavoidable at higher fiber contents. This effect can be further amplified by microstructural defects, such as interfacial gaps formed during manual processing, which provide continuous pathways for water diffusion. These findings also provide important context for the flexural performance under wet conditions, where moisture exposure may induce fiber swelling and weaken interfacial bonding, thereby reducing load transfer efficiency.

### 3.3. Tensile testing

Fig. 3c presents the tensile strength of neat rHDPE and rHDPE composites reinforced with short sugar palm fibers. A progressive increase in tensile strength is observed with increasing fiber loading across the investigated range. Neat rHDPE (0 wt% fiber) exhibited a tensile strength of 11.52 MPa, which increased to 13.91 MPa (10 wt%), 17.80

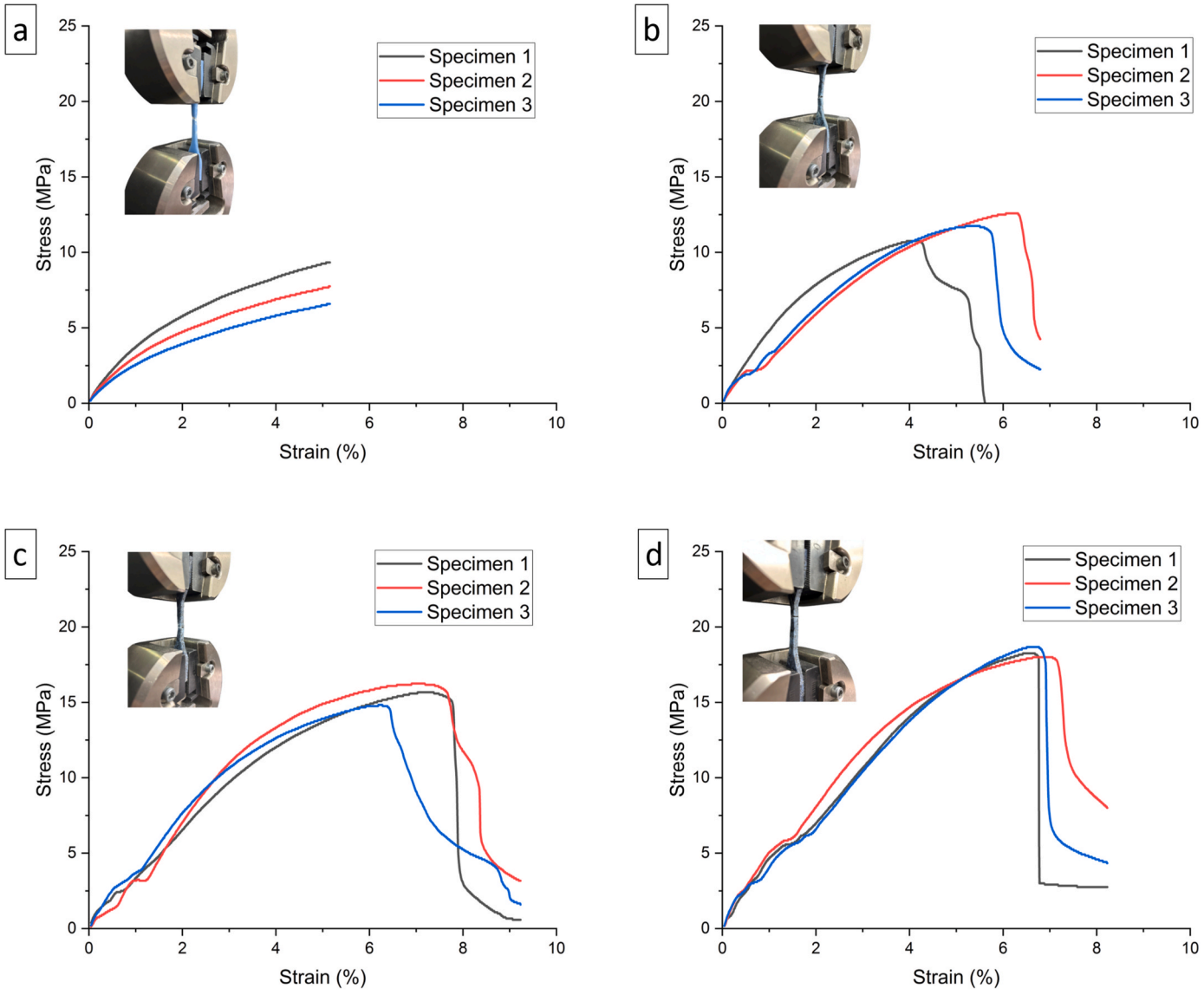


**Fig. 4.** Representative tensile stress-strain curves of sugar palm fiber-reinforced recycled high-density polyethylene bottle-cap composites at different fiber loadings: (a) 0 wt%, (b) 10 wt%, (c) 15 wt%, and (d) 20 wt%.

MPa (15 wt%), and 20.92 MPa (20 wt%).

The introduction of 10 wt% sugar palm fiber resulted in an increase of 2.38 MPa (20.7%) relative to neat rHDPE. Increasing the fiber content from 10 to 15 wt% produced the largest increment, with a gain of 3.90 MPa (28.0% relative to the 10 wt% composite). A further increase from 15 to 20 wt% yielded an additional improvement of 3.12 MPa (17.5% relative to 15 wt%). Overall, the tensile strength increased by 9.40 MPa from 0 to 20 wt%, corresponding to a total improvement of 81.5%. To further illustrate the effect of fiber loading on tensile deformation behavior, the corresponding stress–strain curves for each formulation are presented in Fig. 4.

The addition of palm fibers showed a tendency to increase the tensile load-bearing capacity as well as changes in deformation and fracture modes that were more influenced by microstructural heterogeneity [47–49]. Quantitatively, the tensile strength increased from 11.52 MPa (0 wt%) to 13.91 MPa (10 wt%), 17.80 MPa (15 wt%), and 20.92 MPa (20 wt%), which is consistent with a load-sharing mechanism where well-dispersed and embedded fibers carry the load and enhance stress transfer from the rHDPE matrix to the fiber phase. The effectiveness of this load-sharing mechanism can be largely attributed to the alkali modification of sugar palm fibers. Consistent with previous findings [20], NaOH treatment successfully removes surface impurities, waxes, and partial hemicellulose. This process significantly enhances the surface roughness of the fibers, thereby promoting stronger mechanical interlocking and superior interfacial stress transfer within the hydrophobic rHDPE matrix. However, the stress-strain curves showed that the fibrous composites tended to achieve higher stress with lower breaking strain than pure rHDPE, indicating the effect of fiber constraint on matrix plastic deformation; the differences between the S1–S3 curves in each formulation also suggest local variations (fiber dispersion/orientation, microgap/void) that may cause some specimens to fail premature [49]. This context is in line with SEM, rHDPE without fibers shows a relative smoother fracture surface with typical recycled micro-heterogeneity features that have the potential to initiate cracks, while the fibrous composites show a rougher and non-uniform surface that suggests a more tortuous crack path and the involvement of fiber-related mechanisms such as matrix tearing around the fibers, crack deflection, and possible local debonding and pull-out [50]. The increase in tensile strength is main related to the contribution of fiber reinforcement, while the changes in the curve shape and fracture morphology confirm that the tensile response remains sensitive to the dispersion/interface quality and microstructural non-uniformities in the rHDPE–palm fiber composites [51].

### 3.4. Flexural testing under dry and wet conditions

Under dry conditions, neat rHDPE (0 wt% fiber) exhibited a flexural strength of 45.09 ± 1.32 MPa. Introducing 10 wt% sugar palm fibers reduced the flexural strength to 40.80 ± 0.97 MPa, corresponding to a decrease of 4.29 MPa (−9.51%) relative to neat rHDPE. A further reduction was observed at 15 wt%, where flexural strength decreased to 37.56 ± 5.64 MPa, i.e., 7.53 MPa lower (−16.70%) than the 0 wt% formulation. In contrast, the composite containing 20 wt% fiber showed a higher mean flexural strength of 56.87 ± 12.37 MPa, representing an increase of 11.78 MPa (+26.13%) compared with neat rHDPE. To evaluate moisture-related changes in flexural behavior, dry and water-conditioned flexural strengths and the associated retention/loss values were analyzed, as shown in Fig. 5.

Overall, the dry flexural response exhibited a non-linear trend across the investigated fiber loadings. The relatively large scatter observed at 20 wt%, as reflected by the higher standard deviation, suggests increased inter-specimen variability at this loading. This variability may be associated with differences in fiber distribution, local consolidation, and void formation, which are inherent to manual premixing and hot-pressing processes [52]. Accordingly, the apparent improvement observed at 20 wt% should be interpreted with caution and considered alongside the corresponding load–displacement behavior, as well as fracture and morphological observations. This combined analysis is necessary to assess whether the observed enhancement is consistently achieved across specimens. Table 4 presents the flexural strength results measured in dry and water-conditioned states for all fiber loadings, including the calculated wet/dry retention and strength loss.

Under wet conditions, the flexural strength values remained within a relatively narrow range: 23.52 ± 3.84 MPa (0 wt%), 25.80 ± 4.02 MPa (10 wt%), 23.80 ± 1.97 MPa (15 wt%), and 24.65 ± 2.22 MPa (20 wt%). Compared to the dry state, all formulations exhibited notable reductions in flexural strength, amounting to 47.84% (0 wt%), 36.75%

**Table 4**
Flexural strength of rHDPE/sugar palm fiber composites under dry and wet conditions, including wet/dry retention and strength loss.

| Sugar palm fiber loading (wt%) | Flexural strength (Dry) (MPa) | Flexural strength (Wet) (MPa) | Retention (Wet/Dry) (%) | Loss (%) |
|---|---|---|---|---|
| 0 | 45.09 ± 1.32 | 23.52 ± 3.84 | 52.16 | 47.84 |
| 10 | 40.80 ± 0.97 | 25.81 ± 4.02 | 63.25 | 36.75 |
| 15 | 37.56 ± 5.64 | 23.80 ± 1.97 | 63.35 | 36.65 |
| 20 | 56.87 ± 12.37 | 24.65 ± 2.22 | 43.35 | 56.65 |

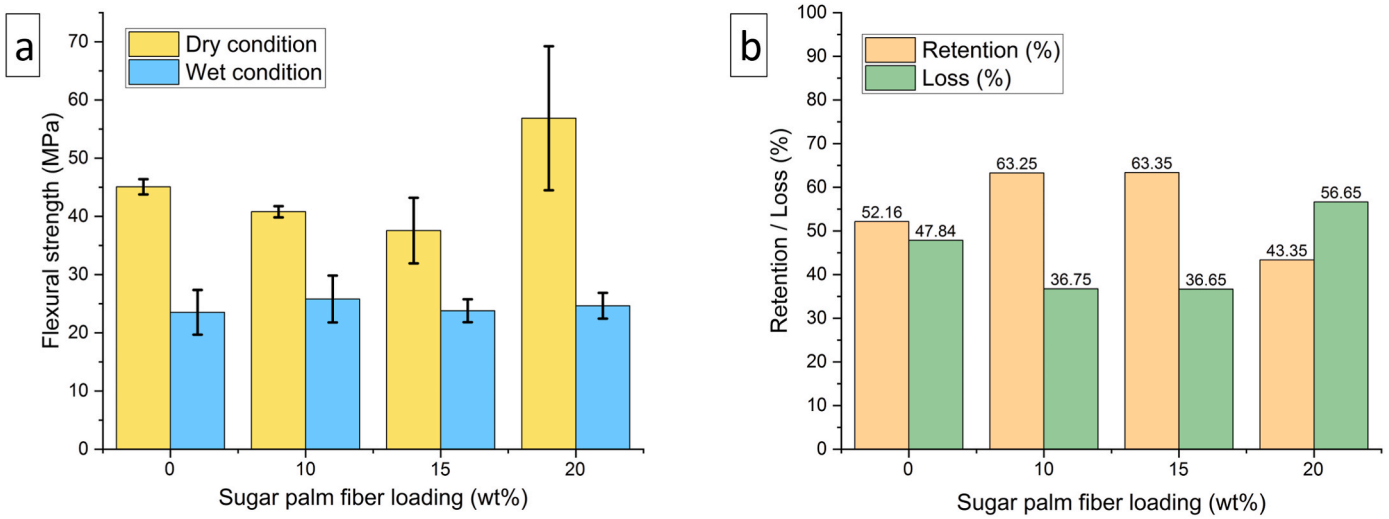


**Fig. 5.** (a) Flexural strength in dry and wet conditions versus sugar palm fiber loading. (b) Wet/dry strength retention and loss versus sugar palm fiber loading.

(10 wt%), 36.65% (15 wt%), and 56.65% (20 wt%). When expressed in terms of wet/dry strength retention, the corresponding values were 52.16%, 63.25%, 63.35%, and 43.35%, respectively. These results indicate that, under the applied water-conditioning and testing conditions, the composites with 10–15 wt% fiber loading retained a greater proportion of their flexural strength compared to the 0 wt% and 20 wt% formulations. The flexural load–displacement responses in the dry condition are presented in Fig. 6.

This behavior can be interpreted in conjunction with the 24 h water absorption results, which showed a progressive increase in moisture uptake with increasing fiber content. Moisture exposure is known to reduce flexural performance through mechanisms such as fiber swelling and diminished interfacial efficiency, effects that may become more pronounced in composites with higher interfacial area and the presence of local defects. However, given that the wet flexural strengths remain relatively similar across all formulations while the corresponding dry strengths differ substantially, it is not possible to attribute the observed retention differences to a single dominant mechanism based solely on mechanical data [52]. Additional evidence, such as fracture-surface morphology or void assessment, would be needed to clarify the relative contributions of interfacial weakening, microvoids, and fiber dispersion at each loading. Fig. 7 presents the wet-condition load–displacement curves for the composites.

### 3.5. Impact test

The Charpy impact strength results (Fig. 8a) show that neat rHDPE (0 wt% fiber) exhibited an impact strength of 11.38 ± 1.11 kJ/m$^2$. With fiber addition, the impact strength increased to 13.46 ± 3.00 kJ/m$^2$ at 10 wt% and reached the highest mean value of 15.75 ± 1.31 kJ/m$^2$ at 15 wt%, before decreasing to 9.02 ± 0.99 kJ/m$^2$ at 20 wt%.

Quantitatively, the increase from 0 to 10 wt% corresponds to +2.08 kJ/m$^2$ (+18.27%), and from 10 to 15 wt% an additional +2.29 kJ/m$^2$ (+17.02%). Overall, the composite containing 15 wt% fiber exhibited an increase in impact strength of +4.37 kJ/m$^2$ (+38.39%) compared to neat rHDPE. In contrast, further increasing the fiber content to 20 wt% resulted in a significant reduction of −6.73 kJ/m$^2$ (−42.73%), yielding a value 20.74% lower than that of the unreinforced matrix.

The improvement observed up to 15 wt% suggests that moderate fiber content enhances the ability of the composite to absorb impact energy relative to the matrix alone. Within the investigated range, this result indicates that the reinforcement effect under impact loading is not monotonic, and that an intermediate fiber loading provides the most favorable response.

The drop in impact strength at 20 wt% suggests that this increased fiber loading may render the composite more sensitive to processing-related variation, particularly when local heterogeneity and interfacial

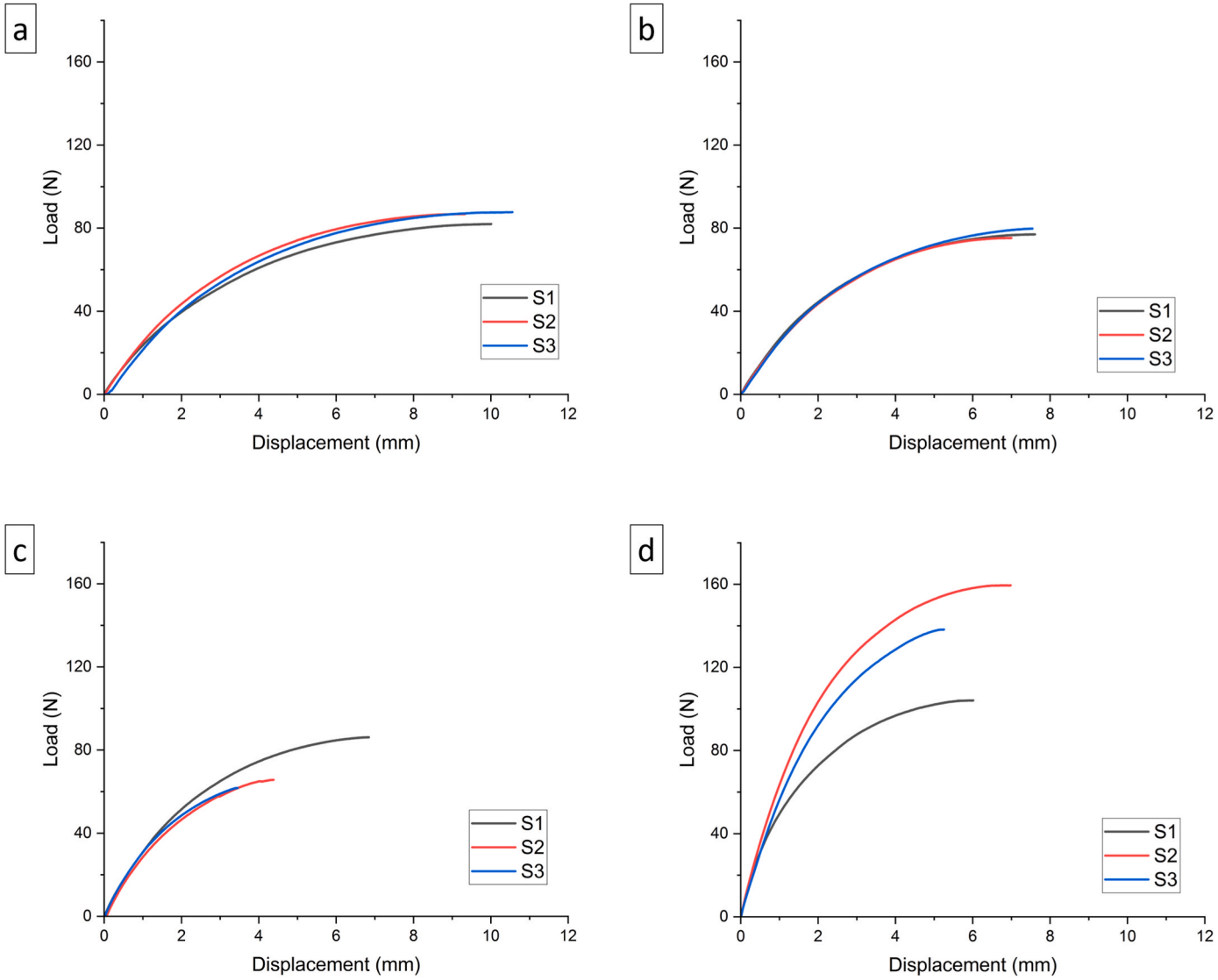


**Fig. 6.** Load–displacement curves (dry condition) of rHDPE/sugar palm fiber composites at (a) 0 wt%, (b) 10 wt%, (c) 15 wt%, and (d) 20 wt% fiber loading.

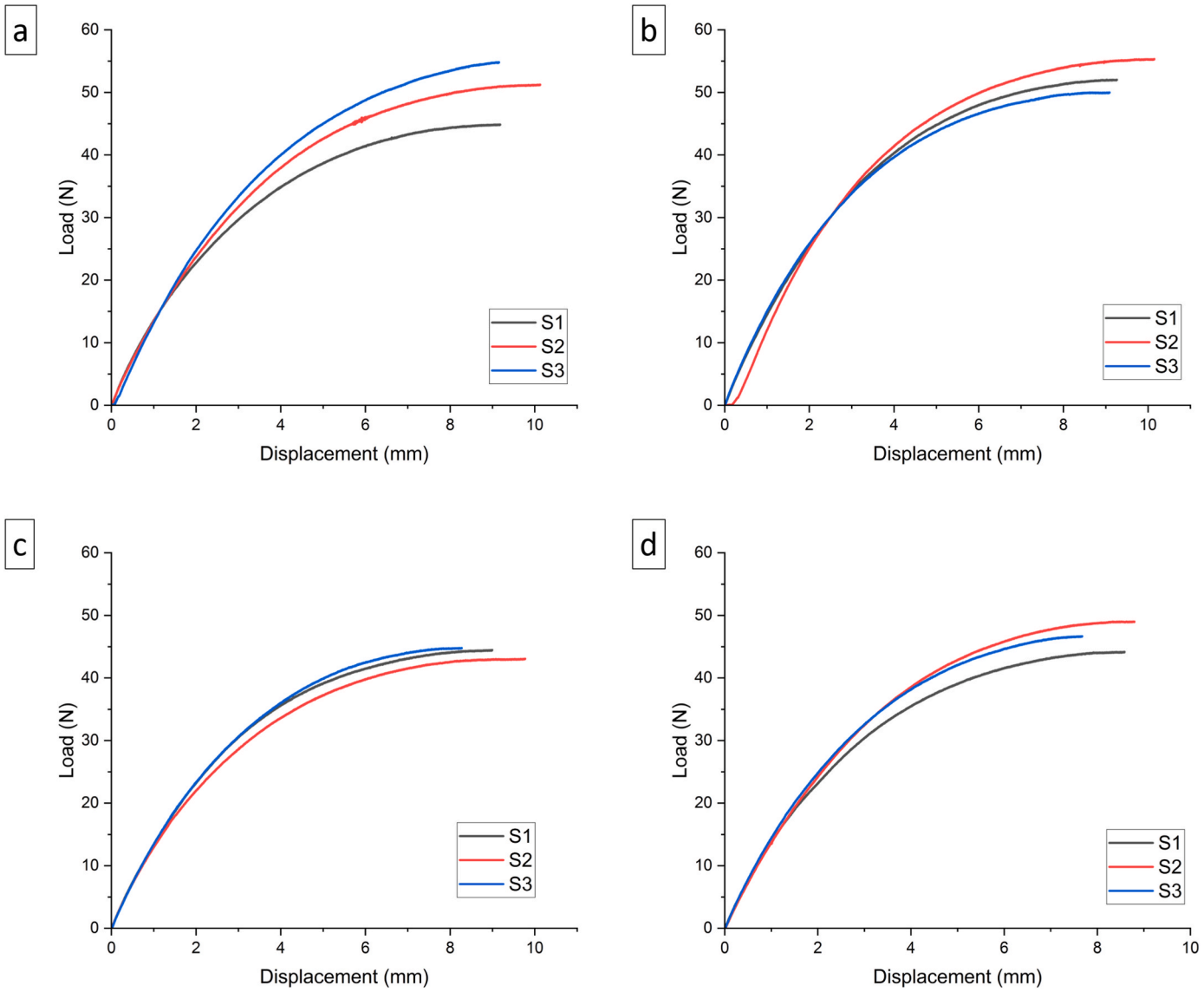


**Fig. 7.** Load–displacement curves (wet condition) of rHDPE/sugar palm fiber composites at (a) 0 wt%, (b) 10 wt%, (c) 15 wt%, and (d) 20 wt% fiber loading.

features influence crack initiation and energy absorption [53,54]. This study shows that increasing fiber contents are associated with asymmetric distribution of the fibers in hot-pressed matrix leading to incomplete wetting of the fibers in high density regions producing voids. Such properties may act as stress raisers under impact loading, degrading the effect of the composite to a fast fracture. Consequently, impact testing results demonstrate that formulation containing 15 wt% fiber strikes an ideal balance of impact protection from the formulations assessed experimentally [54,55]. However, definitive identification of the underlying fracture-related mechanisms would require dedicated fracture toughness testing and impact-specific fractographic analysis, which were outside the scope of the present study.

### 3.6. Hardness test

Hardness (Shore D) increased progressively with increasing sugar palm fiber loading, from 53.70 for neat rHDPE to 55.90 (10 wt%), 59.10 (15 wt%), and 60.10 (20 wt%). The composite containing 20 wt% fiber exhibited an overall increase of 6.40 Shore D units, corresponding to an improvement of 11.92% relative to neat rHDPE. The most significant incremental increase was observed between 10 and 15 wt% (+3.20 units), whereas the gain from 15 to 20 wt% was comparatively smaller (+1.00 unit), indicating a diminishing marginal effect at higher fiber loadings. Fig. 8b summarizes the Shore D hardness values measured for rHDPE/sugar palm fiber composites with varying fiber contents.

This trend is consistent with a constraint effect during indentation, whereby the presence of a relatively rigid lignocellulosic phase restricts local plastic deformation of the rHDPE matrix and enhances resistance to the indenter. As Shore D hardness reflects localized, near-surface deformation, it can increase even when other properties particularly those sensitive to defects and crack initiation did not exhibit the same level of improvement. In the present study, both hardness and tensile strength increased with fiber content, whereas impact strength reached a maximum at intermediate loading and declined at 20 wt%. This divergence reflects the differing sensitivities of these properties: impact performance is highly influenced by stress concentrators and microstructural heterogeneities, while hardness is primarily governed by local resistance to indentation. Consistent with this interpretation, fracture surface observations reveal increasingly heterogeneous features at higher fiber loadings, which may contribute to the reduced impact resistance despite continued gains in hardness.

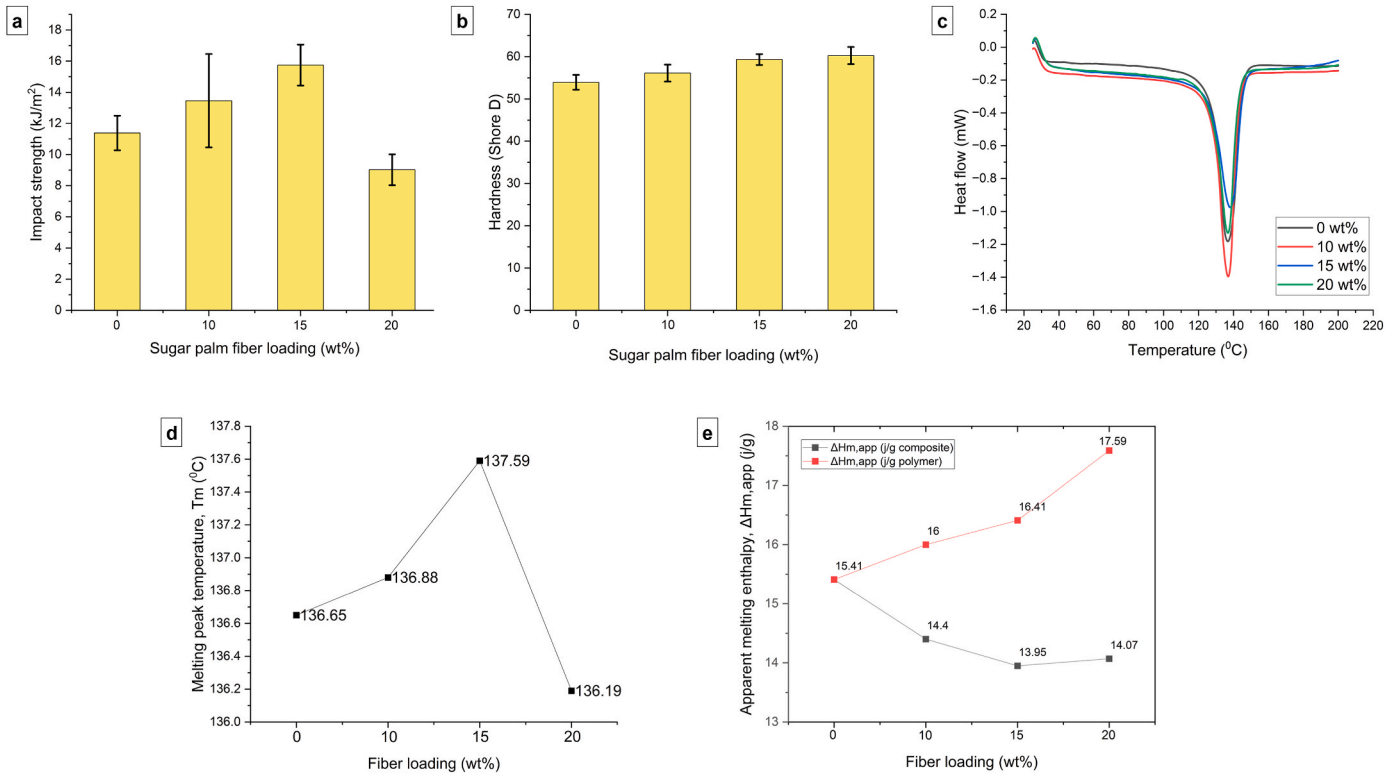


**Fig. 8.** Impact, hardness, and thermal properties of sugar palm fiber-reinforced recycled high-density polyethylene bottle-cap composites at different fiber loadings: (a) Charpy impact strength, (b) Shore D hardness, (c) differential scanning calorimetry heating curves, (d) melting peak temperature, and (e) apparent melting enthalpy of the polymer phase and the composite.

### 3.7. DSC

Fig. 8c presents the DSC heating curves (25–200 °C) of neat rHDPE and rHDPE/sugar palm fiber composites. The corresponding melting peak temperature (Tm) and apparent melting enthalpy (ΔHm,app) are summarized in Fig. 8d and e. The melting peak temperature exhibited only minor variation across the different formulations, remaining within a narrow range of 136.19–137.59 °C. This indicates that, within the investigated fiber loading range (0–20 wt%), the melting behavior of the rHDPE phase was not significantly affected by the incorporation of sugar palm fibers. Accordingly, the differences in mechanical performance are more plausibly attributed to composite-related factors such as the reinforcing contribution of the fibers and variations in microstructure (fiber dispersion, voids, and interfacial efficiency) rather than a substantial change in the matrix melting temperature [56].

The melting enthalpy is reported as an apparent melting enthalpy (ΔHm,app) to enable relative comparison among formulations. When expressed per gram of composite, ΔHm,app decreased with increasing fiber loading, which is expected because the polymer fraction decreases as the fiber fraction increases. After normalization by the rHDPE mass fraction, ΔHm,app expressed per unit polymer showed an increasing trend across the investigated range, indicating that the integrated melting endotherm per unit polymer differs among formulations [57].

However, because the present analysis is based on a heating scan and enthalpy integration can be influenced by baseline selection and thermal history, the ΔHm,app values are interpreted conservatively as comparative thermal indicators rather than definitive crystallinity values. Overall, the DSC results confirm that the melting transition temperature of the rHDPE phase remains stable upon fiber addition, while variations in melting enthalpy provide supporting context for formulation-dependent differences without indicating a single dominant mechanism.

### 3.8. FTIR

The FTIR spectra obtained under dry conditions confirms the coexistence of the rHDPE matrix and lignocellulosic sugar palm fibers within the composites. The spectrum of neat rHDPE (0 wt%) is dominated by characteristic polyethylene bands, including strong C–H stretching vibrations at approximately 2915 and 2848 $cm^{-1}$, along with typical absorption bands in the lower wavenumber region. With increasing sugar palm fiber content (10–20 wt%), additional absorption bands associated with lignocellulosic constituents become progressively more pronounced. A broad O–H stretching band in the 3200–3600 $cm^{-1}$ region indicates the presence of hydroxyl groups. Furthermore, an absorption band around 1730 $cm^{-1}$ is attributed to carbonyl (C═O) functionalities, commonly associated with hemicellulose. The bands observed in the 1600–1510 $cm^{-1}$ range correspond to aromatic C═C vibrations, reflecting the presence of lignin structures. In addition, C–O stretching bands within the 1000–1150 $cm^{-1}$ region confirm the presence of polysaccharide frameworks in the lignocellulosic fibers. Fig. 9 shows the FTIR spectra of the rHDPE/sugar palm fiber composites, highlighting characteristic bands associated with the rHDPE matrix and lignocellulosic fibers.

The progressive intensification of fiber-associated bands with increasing fiber content is consistent with the higher proportion of the sugar palm phase within the composites. Nevertheless, since the spectra predominantly represent a superimposed response from both matrix and fiber constituents, the FTIR results are more appropriately interpreted as evidence of compositional variation rather than definitive proof of newly formed chemical interactions at the fiber–matrix interface.

Although FTIR measurements were conducted on dry specimens, the increasingly pronounced hydroxyl- and C–O-related bands at higher fiber loadings provide useful insight into the moisture sensitivity observed after water conditioning. Water absorption increased from 0.000% (0 wt%) to 0.397% (10 wt%), 1.053% (15 wt%), and 1.164%

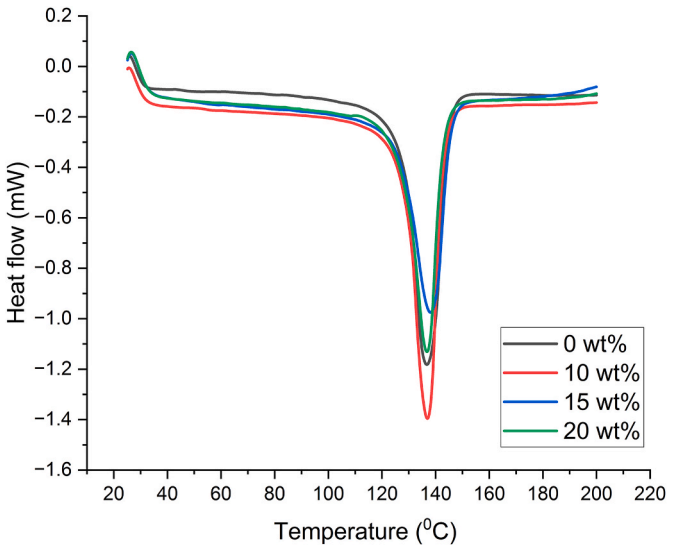


**Fig. 9.** FTIR spectra of sugar palm fiber-reinforced recycled high-density polyethylene bottle-cap composites.

(20 wt%), consistent with the incorporation of a more polar lignocellulosic phase enriched in hydroxyl functionalities. Under flexural loading, wet-condition strengths remained within a relatively narrow range (23.52–25.80 MPa), whereas wet/dry retention increased from 52.16% (0 wt%) to 63.25–63.35% (10–15 wt%) before declining to 43.35% at 20 wt%. Notably, the difference in water absorption between 15 and 20 wt% is relatively small (1.053% to 1.164%), indicating that the reduced retention at 20 wt% cannot be attributed solely to total moisture uptake. Instead, it reflects the way water interacts with the composite microstructure at higher fiber contents, where increased interfacial areas and local heterogeneities may reduce interfacial efficiency under bending.

These moisture-related trends are broadly consistent with the mechanical response. Tensile strength and Shore D hardness increased with fiber loading, reflecting the incorporation of a stiffer reinforcing phase into the ductile rHDPE matrix. In contrast, impact strength improved up to 15 wt% but declined at 20 wt%, indicating a greater sensitivity of impact performance to microstructural features that promote crack initiation and unstable fracture at higher fiber contents. Fractographic observations at 20 wt% support this interpretation, revealing increased heterogeneity, including fiber-rich regions, pull-out features, and void-like cavities. Such characteristics highlight the need for cautious interpretation of the 20 wt% results, particularly for properties governed by interfacial load transfer and fracture resistance. Overall, the FTIR results primarily indicate an increasing contribution of hydrophilic lignocellulosic constituents with rising fiber content, while the combined water absorption and wet flexural retention responses emphasize the growing influence of moisture and microstructural factors at higher loadings [44, 45].

### 3.9. Scanning electron microscopy (SEM)

The SEM images shown in Fig. 10 relate to the fracture surfaces of the tested specimens. The fracture surface of the recycled high-density polyethylene looks neat (Fig. 10a and b) and relatively compact with more homogenization however localized roughness and micro-irregularity can still be seen due to heterogeneous nature of recycled polymer matrices. Upon fiber incorporation, the tensile fracture surface of a composite with 20 wt% sugar palm fiber (Fig. 10c and d) is greatly heterogeneous. Exposed fiber cross-sections, partially embedded fibers, and matrix regions adhering to the fiber surface can be observed, indicating that the fibers participated in load transfer before failure. At the same time, the presence of interfacial gaps and locally detached regions suggests incomplete interfacial continuity in some areas.

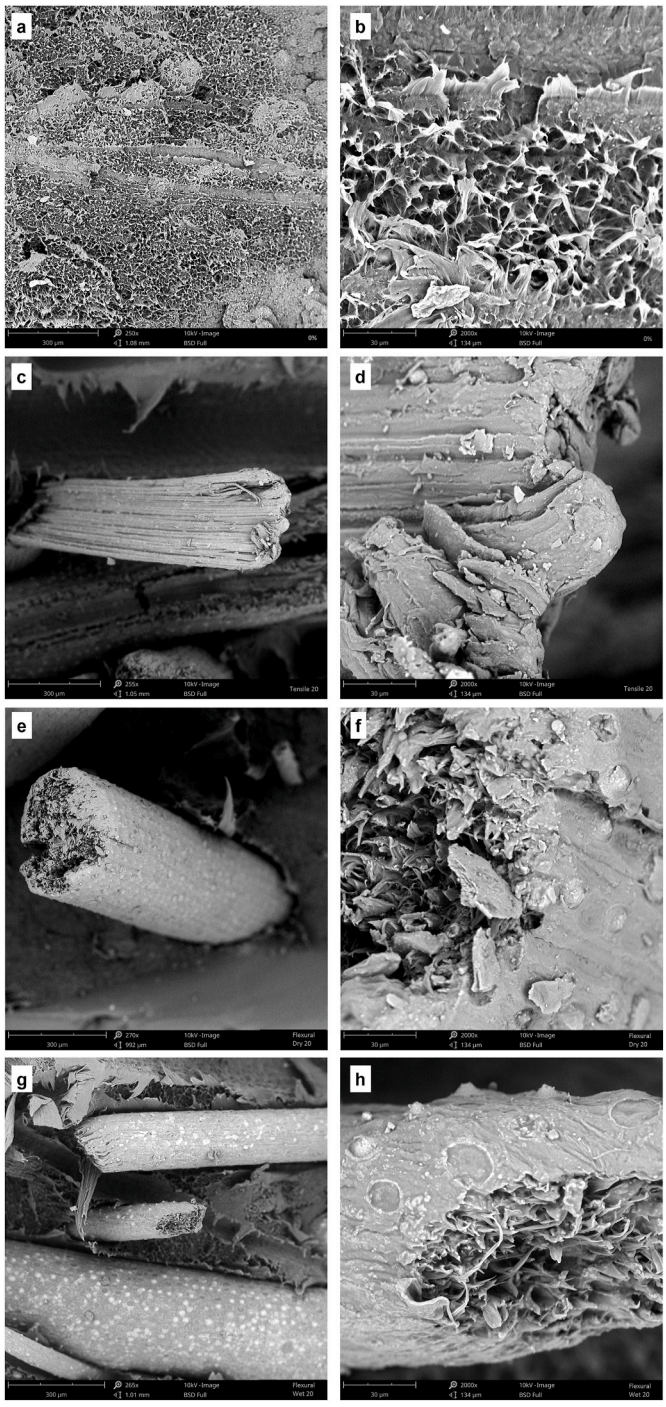


**Fig. 10.** SEM micrographs of fracture surfaces of recycled HDPE/sugar palm fiber composites: (a,b) tensile fracture surface of neat rHDPE (0 wt%), (c,d) tensile fracture surface of the composite containing 20 wt% fiber, (e,f) dry flexural fracture surface of the composite containing 20 wt% fiber, and (g,h) water-conditioned flexural fracture surface of the composite containing 20 wt% fiber, shown at low and high magnifications, respectively.

The flexural fracture surfaces of the 20 wt% composite further reveal the influence of loading and conditioning environment. Under dry flexural conditions (Fig. 10e and f), the fractured surface shows broken fibers surrounded by plastically deformed matrix regions, together with rough and irregular topography. This morphology is consistent with fiber involvement in the fracture process and with localized matrix

tearing around the reinforcement. In contrast, the water-conditioned flexural fracture surface (Fig. 10g and h) exhibits a more disrupted interface, with clearer separation between fiber and matrix, more visible void-like regions, and a less cohesive surrounding matrix morphology. These features suggest that moisture exposure reduced the effectiveness of fiber-matrix interaction and promoted interfacial deterioration. Overall, the SEM observations support the mechanical results by showing that fiber addition increases fracture-surface heterogeneity and fiber participation in failure, while moisture conditioning intensifies interfacial disruption, which is consistent with the reduced flexural strength retention under wet conditions.

### *3.10. Limitations and recommendations for future research*

Although this study demonstrates the reinforcing potential of alkali-treated sugar palm fibers in a recycled HDPE matrix, several limitations should be acknowledged to guide future work. The composites were fabricated via manual premixing followed by hot pressing, which inherently limits process control and reproducibility. Future investigations should therefore consider more controlled and scalable compounding techniques, supported by quantitative characterization of microstructure and porosity as well as predictive approaches for correlating formulation and processing variables with mechanical performance [58], such as twin-screw extrusion or injection molding, supported by quantitative characterization of microstructure and porosity. In addition, the inclusion of fracture toughness measurements would provide a more rigorous basis for elucidating the underlying energy-dissipation mechanisms during impact and fracture.

Furthermore, alkali treatment was employed as the sole fiber modification strategy in this study. To further reduce moisture uptake and enhance interfacial load transfer, future research should explore the use of compatibilizer agents, such as maleic anhydride-grafted polyethylene (MAPE), in combination with optimized processing conditions. Such approaches are expected to improve wet-conditioning retention and enhance fracture-related performance in lignocellulosic fiber reinforced composites.

## 4. Conclusion

Incorporating short sugar palm fibers provides a practical and sustainable route for tailoring recycled HDPE bottle-cap composites produced by manual mixing and hot pressing. The performance of the composites is significantly influenced by fiber loading and moisture exposure. Overall, alkali-treated sugar palm fiber loadings in the range of 10–15 wt% provide the most favorable overall balance between impact resistance and wet-condition flexural retention. The findings also suggest a compromise. Specifically, increasing fiber content can improve certain mechanical properties when the material is dry, but it also makes the material more vulnerable to water. Consequently, the optimal fiber loading must be determined based on the specific operational environment and the desired performance attributes.

## Declaration of competing interest

The authors declare that they have no known competing financial interests or personal relationships that could have appeared to influence the work reported in this paper.

## Acknowledgments

This work was funded by the Enhancing Quality Education for International University Impacts and Recognition Times Higher Education Impact Rankings 2025 (EQUITY 2025) Program, Directorate of Institutional Affairs, Directorate-General of Higher Education, Ministry of Higher Education, Science, and Technology of the Republic of Indonesia. Contract No. 4311/B3/DT.03.08/2025 under grant number of 2.11.11/UN37/PPK.R01/2025.

## References

[1] Issakah O, Kayaba AM, Fiagbe Y, Akromah S, Kpare JY, Asare EKA. Effect of partial replacement of CaCO3 with palm kernel shell particles on the mechanical properties of PKS/CaCO3/HDPE hybrid composites. Results Mater 2025;25:100668. https://doi.org/10.1016/j.rinma.2025.100668.

[2] Daniele R, Armoni D, Dul S, Alessandro P. From nautical waste to additive manufacturing: sustainable recycling of high-density polyethylene for 3D printing applications. J Compos Sci 2023;7. https://doi.org/10.3390/jcs7080320.

[3] Dun M, Wang W, Fu H, Hao J. Strategies for improving the strength, toughness, and winding properties of sisal fiber/polyethylene pre-preg tape. J Mater Res Technol 2025;36:5675–83. https://doi.org/10.1016/j.jmrt.2025.04.218.

[4] Liang J, Wang J, Qin S. Super toughness and reinforcement of recycled high-density polyethylene/poly (ethylene terephthalate) composite achieved by oriented spherical crystal structure. Compos Part B 2025;294:112158. https://doi.org/10.1016/j.compositesb.2025.112158.

[5] Hasan MM, Rahman MZ, Ahmed RS, Hossain MFT, Dewan MW. Development and characterization of jute-pineapple leaf fiber reinforced PLA hybrid composites: effect of chemical treatments on mechanical properties and environmental durability. J Mater Res Technol 2026;40:4063–76. https://doi.org/10.1016/j.jmrt.2025.11.238.

[6] Huang B, Yu Y, Yang Z, Wang Y, Wang J, Zuo L, Yu H, Wang D, Wang X, Sun J. Recycled expanded polystyrene foam utilization in 3D-Printed fiber-reinforced concrete. J Mater Res Technol 2025;39:4204–16. https://doi.org/10.1016/j.jmrt.2025.10.113.

[7] Kacem MA, Guebailia M, Dezaki ML, Abdi S, Sabba N, Zolfagharian A, Bodaghi M. Development and 3D printing of PLA bio-composites reinforced with short yucca fibers and enhanced thermal and dynamic mechanical performance. J Mater Res Technol 2025;36:1243–58. https://doi.org/10.1016/j.jmrt.2025.03.184.

[8] Shaik MS, Subramanian HS, B RK, Suyambulingam I, Senthamaraikannan P, Kumar R. A review on fiber properties, manufacturing, and crashworthiness of natural fiber-reinforced composite structures. J Nat Fibers 2025;22:2520845. https://doi.org/10.1080/15440478.2025.2520845.

[9] Nuryanta MI, Widodo RD, Mujaki A, Rusiyanto Kriswanto, Widayat W, Fitriyana DF, Firmansyah HN, Darsono FB, Muflikhun MA. The effect of stacking sequence on the properties of hybrid agel/glass fiber reinforced polymer composite laminates. IOP Conf Ser Earth Environ Sci 2024;1381:4–10. https://doi.org/10.1088/1755-1315/1381/1/012014.

[10] Mulenga TK, Rangappa SM, Lai CW, Anam K, Moure MM, Siengchin S. Synergistic performance in natural fiber hybrid composites: a review of weathering, thermal, and mechanical properties through filler integration. J Mater Res Technol 2026;40:662–78. https://doi.org/10.1016/j.jmrt.2025.12.077.

[11] Hidalgo-Salazar MA, Correa-Aguirre JP, Román AJ, Gonzalez R, Vera R, Osswald TA. Colombian natural fibers: potential applications in sustainable natural fiber reinforced composites materials. Polym Compos 2025;46:5599–617. https://doi.org/10.1002/pc.29313.

[12] Bonyani M, Marincic IC, Krishnan S. Advancing sustainable materials engineering with natural-fiber biocomposites. J Compos Sci 2026;10. https://doi.org/10.3390/jcs10020086.

[13] Widodo RD, Nuryanta MI, Fitriyana DF, Rusiyanto, Firmansyah HN, Widayat W, Kriswanto, Darsono FB, Mujaki A, Muflikhun MA. The influence of flex banner types on the impact and flexural strength of hybrid composite materials. J Phys, Conf Ser 2025;3103:12035. https://doi.org/10.1088/1742-6596/3103/1/012035.

[14] Almeida LM, Rios da Silva AC, Duarte Lopes FP, Simonassi NT, Monteiro SN, Candido VS. Caranan fibers (Mauritiella armata) and new reinforcements of polyester composites with natural fibers functionalized with graphene oxide and their application potential. J Mater Res Technol 2025;34:2232–52. https://doi.org/10.1016/j.jmrt.2024.12.233.

[15] Imraan M, Ilyas RA, Norfarhana AS, Bangar SP, Knight VF, Norrrahim MNF. Sugar palm (Arenga pinnata) fibers: new emerging natural fibre and its relevant properties, treatments and potential applications. J Mater Res Technol 2023;24:4551–72. https://doi.org/10.1016/j.jmrt.2023.04.056.

[16] Thimmegowda DY, Hindi J, Markunti GB, Kakunje M. Enhancement of mechanical properties of natural fiber reinforced polymer composites using different Approaches—A review. J Compos Sci 2025;9. https://doi.org/10.3390/jcs9050220.

[17] Nuryanta MI, Aryaswara LG, Korsmik R, Klimova-Korsmik O, Nugraha AD, Darmanto S, Kusni M, Muflikhun MA. The interconnection of carbon active addition on mechanical properties of hybrid Agel/Glass fiber-reinforced green composite. Polymers 2023;15. https://doi.org/10.3390/polym15112411.

[18] Khan A, Sapuan SM, Zainudin ES, Zuhri MYM. Hybridization and its transformative role in bamboo fiber reinforced polymer composites: a review. Adv Compos Hybrid Mater 2024;7:164. https://doi.org/10.1007/s42114-024-00974-8.

[19] Widodo RD, Nuryanta MI, Handayani PA, Ichwan R, Zainudin ES, Muflikhun MA. Sustainable hybrid laminated composites reinforced with bamboo, flex banner, and glass fibers: impact of CaCO3 filler on mechanical properties. Polymers 2026;18. https://doi.org/10.3390/polym18020275.

[20] Widodo E, Pratikto Sugiarto, Widodo TD. Comprehensive investigation of raw and NaOH alkalized sansevieria fiber for enhancing composite reinforcement. Case Stud Chem Environ Eng 2024;9:100546. https://doi.org/10.1016/j.cscee.2023.100546.

[21] Awad SA, Awayssa O, Jawaid M, Ismail AS, Saba N, Yaseen M, Sain M, Fouad H. Performance enhancement of hybrid kenaf/bamboo fibre-reinforced bio-epoxy

composites for sustainable structural applications. J Mater Res Technol 2026;41:29–38. https://doi.org/10.1016/j.jmrt.2025.12.017.
[22] Zhu C, Zhang S, Li D, Chen X, Guo J, Jiao H. Mechanical behavior and toughening mechanisms of polypropylene fiber-reinforced shotcrete: a combined experimental and simulation study. J Mater Res Technol 2025;38:3712–33. https://doi.org/10.1016/j.jmrt.2025.08.110.
[23] Kiran U, Nath H, Brito FP, Fangueiro R. Industrial Crops & Products A comparative evaluation of alkaline surface treatment impact on the structural , mechanical and thermal properties of natural plant fibers. Ind Crop Prod 2026;242:122860. https://doi.org/10.1016/j.indcrop.2026.122860.
[24] Olanrewaju O, Oladele IO, Adelani SO. Recent advances in natural fiber reinforced metal/ceramic/polymer composites: an overview of the structure-property relationship for engineering applications. Hybrid Adv 2025;8:100378. https://doi.org/10.1016/j.hybadv.2025.100378.
[25] Fahmida-E-Karim, Ara Begum H, Islam MR. Natural Fiber-Reinforced, natural resin-based biocomposites: fabrication, properties, and sustainable applications. Adv Mater Sci Eng 2026;2026:1139054. https://doi.org/10.1155/amse/1139054.
[26] Nuryanta MI, Nurhary MA, Firmansyah HN, Joshua D, Hajad M, Widodo RD, Widodo TD, Kusni M, Wiranata A, Kusumawanto A, Muflikhun MA. Optimization of Kaolin clay composition for enhanced mechanical properties in 3D-Printed structures. Constr Mater 2025;5. https://doi.org/10.3390/constrmater5040083.
[27] Dubey SC, Patil S, Mishra V, Sharma A. Agricultural waste fiber/filler composites: a review on physical, mechanical and wear behaviour. Discov Appl Sci 2025;8:10. https://doi.org/10.1007/s42452-025-07911-4.
[28] Gonzalez CS, Nouvel C, Pearce JM. Multi-material distributed recycling via material extrusion : recycled high density polyethylene and poly (ethylene terephthalate) mixture. 1555–1570, https://doi.org/10.1002/pen.26643; 2024.
[29] Fazli A, Stevanovic T, Rodrigue D. Recycled HDPE/Natural fiber composites modified with waste tire rubber: a comparison between injection and compression molding. Polymers 2022;14. https://doi.org/10.3390/polym14153197.
[30] Espinach FX, Monzon M, Paz R, Ortega R, Fullana P, Bala A, Campos C. Composites made of a blend of plastics recovered from bottle caps reinforced with fibers from banana rachis waste. A Circular Economy Strategy in the Canary Islands 2025:483. https://doi.org/10.1016/j.jclepro.2024.144244.
[31] Ming L, He H, Li X, Tian W, Zhu C. Study of the effect of NaOH treatment on the properties of GF/VER composites using AE technique. Materials 2024;17. https://doi.org/10.3390/ma17061407.
[32] dos Santos AJG, Ribeiro MM, Corrêa A de C, Rodrigues J da S, Silva DS, Junio RFP, Monteiro SN. Investigation of the flexural and tensile properties of hybrid polyester composites reinforced with bamboo fibers and red mud waste. Polymers 2025;17. https://doi.org/10.3390/polym17081060.
[33] Rahman Z, Hannan A, Zahirul M, Mollah I. Heliyon Evaluating physico-mechanical properties of NaOH-treated natural fibres : effects of polyolefin. Heliyon 2024;10:e39673. https://doi.org/10.1016/j.heliyon.2024.e39673.
[34] Ehiosu N, Rusnakova S, Ebele A, Olabanji R, Onyedekachi S, Nosakhare A. A comprehensive review of natural fiber reinforced Polymer composites as emerging materials for sustainable applications. Appl Mater Today 2025;43:102666. https://doi.org/10.1016/j.apmt.2025.102666.
[35] Seid AM, Adimass SA. Heliyon Review on the impact behavior of natural fiber epoxy based composites. Heliyon 2024;10:e39116. https://doi.org/10.1016/j.heliyon.2024.e39116.
[36] Ichim M, Muresan EI, Codau E. Natural-Fiber-Reinforced polymer composites for furniture applications. Polymers 2024;16. https://doi.org/10.3390/polym16223113.
[37] Tong JY, Royan NRR, Ng YC, Ab Ghani MH, Ahmad S. Study of the mechanical and morphology properties of recycled HDPE composite using rice husk filler. Adv Mater Sci Eng 2014;2014:938961. https://doi.org/10.1155/2014/938961.
[38] ASTM International. ASTM D638-22 standard Test method for tensile properties of plastics. 2022. West Conshohocken, PA.
[39] ASTM International. ASTM D790-17 standard Test methods for flexural properties of unreinforced and reinforced plastics and electrical insulating materials. 2017. West Conshohocken, PA.
[40] ASTM International. ASTM D6110-18 standard Test method for determining the charpy impact resistance of notched specimens of plastics. 2018. West Conshohocken, PA.
[41] ASTM International. ASTM D2240-15(2021) standard Test method for rubber Property—Durometer hardness. 2021. West Conshohocken, PA.
[42] ASTM International. ASTM D792-20 standard Test methods for density and specific gravity (relative density) of plastics by displacement. 2020. West Conshohocken, PA.
[43] ASTM International. ASTM D570-98(2018) standard Test method for water absorption of plastics. 2018. West Conshohocken, PA.
[44] Mohammed M, Rahman R, Mohammed AM, Adam T, Betar BO, Osman AF, Dahham OS. Surface treatment to improve water repellence and compatibility of natural fiber with polymer matrix: recent advancement. Polym Test 2022;115:107707. https://doi.org/10.1016/j.polymertesting.2022.107707.
[45] Addis LB, Sendekie ZB, Satheesh N. Degradation kinetics and durability enhancement strategies of cellulosic fiber-reinforced geopolymers and cement composites. Adv Mater Sci Eng 2022;2022:1981755. https://doi.org/10.1155/2022/1981755.
[46] Islam S, Karim F-E-, Islam MR. Assessing the consequences of water retention on the structural integrity of jute fiber and its composites: a review. SPE Polym 2024;5:457–80. https://doi.org/10.1002/pls2.10142.
[47] Kareem A, Mehboob SS, Khan D, Qureshi QB alias IL, Rezzoug A, Hayat K, Ali A, Mumtaz MA. A review on date palm fiber as a sustainable reinforcement for concrete applications. Int J Concr Struct Mater 2025;19:98. https://doi.org/10.1186/s40069-025-00840-x.
[48] Mohanraj CM, Rameshkumar R, Mariappan M, Mohankumar A, Rajendran B, Senthamaraikannan P, Suyambulingam I, Kumar R. Recent progress in fiber reinforced polymer hybrid composites and its Challenges-A comprehensive review. J Nat Fibers 2025;22:2495911. https://doi.org/10.1080/15440478.2025.2495911.
[49] Lakshme Gowda DM, Bhat RS, Rangappa SM, Siengchin S. Review on fiber composites for sustainable high strain rate applications. iScience 2025;28:113598. https://doi.org/10.1016/j.isci.2025.113598.
[50] Patsiaoura D, Tarani E, Bikiaris DN, Pavlidou E, Chrissafis K. Lignocellulosic-Based/High density polyethylene composites: a comprehensive Study on fiber characteristics and performance evaluation. Appl Sci 2024;14. https://doi.org/10.3390/app14093582.
[51] Puneethraj HP, Sharma S, Achutha Kini U, Shettar M, Hegde A, Gowrishankar MC. Impact of fiber treatment and nanoclay addition on water soaking effects of coir fiber reinforced epoxy composites. J Mater Res Technol 2025;39:6286–99. https://doi.org/10.1016/j.jmrt.2025.11.032.
[52] Saha S, Das S, Rahman MZ. Hybridization in natural fiber composites: enhanced performance and sustainability. Composites, Part B Eng 2026;308:112986. https://doi.org/10.1016/j.compositesb.2025.112986.
[53] D. Kumar, B. Kuiri, Amika, D. Kumar, A.S. Chauhan, S.A. Bansal, Experimental and computational investigation of fiber-matrix interactions in glass Fiber/PA6/HDPE tertiary composites for low load-bearing applications, Polym Compos. n/a (n.d.). https://doi.org/https://doi.org/10.1002/pc.70867.
[54] Belhaoues A. Preparation and characterization of a high-density polyethylene/date seed (HDPE/DS) composites: effect of particle size, content, and chemical treatment of the DS powder filler on composite properties. J Compos Mater 2025. https://doi.org/10.1177/00219983251401106. 00219983251401106.
[55] Taj A, Bharath KN, Hiremath A, Madhu P, Sanjay MR, Siengchin S. Mechanical enhancement of sustainable natural fiber composites through filler additives: a comprehensive review. J Umm Al-Qura Univ Eng Archit 2025. https://doi.org/10.1007/s43995-025-00240-y.
[56] K S, Brn M, Hiremath A, Singh MK, Palaniappan SK, Rangappa SM, Siengchin S. Investigation of thermo-mechanical and tribological performance of zirconia-coated MWCNTs reinforced HDPE composites. Constr Build Mater 2025;496:143830. https://doi.org/10.1016/j.conbuildmat.2025.143830.
[57] Tyukanko V, Tarunin R, Demyanenko A, Semenyuk V, Dyuryagina A, Merkibayev Y, Bakibaev A, Alpyssov R, Alyoshin D. Optimization of composite formulation using recycled polyethylene for rotational molding. Polymers 2025;17. https://doi.org/10.3390/polym17243290.
[58] Kumar SS, Shyamala P, Pati PR, Mishra DK, Sharma V, Tank G, Kanan M. Investigation and machine learning-based prediction of mechanical properties in hybrid natural fiber composites. Sci Rep 2025;15:33700. https://doi.org/10.1038/s41598-025-18944-5.

# Update

Journal of Materials Research and Technology
Volume 42, Issue , May - June 2026, Page 6575-6576

DOI: https://doi.org/10.1016/j.jmrt.2026.04.184

Journal of Materials Research and Technology 42 (2026) 6575–6576

Contents lists available at ScienceDirect

Journal of Materials Research and Technology

journal homepage: www.elsevier.com/locate/jmrt

Corrigendum

# Corrigendum to "Property relationships study of sugar palm fiber-reinforced recycled HDPE bottle-cap composites" [J Mater Res Technol 42, May–June 2026, 4311-4323]

Rahmat Doni Widodo [a,*], Muhammad Irfan Nuryanta [a], Prima Astuti Handayani [b], Rizky Ichwan [b], Edi Syams Zainudin [c], Muhammad Akhsin Muflikhun [d]

[a] Department of Mechanical Engineering, Universitas Negeri Semarang, Semarang, Indonesia
[b] Department of Chemical Engineering, Faculty of Engineering, Universitas Negeri Semarang, Semarang, 50229, Indonesia
[c] Advanced Engineering Materials and Composite Research Centre (AEMC), Department of Mechanical and Manufacturing Engineering, Universiti Putra Malaysia, UPM, Serdang, Selangor, 43400, Malaysia
[d] Department of Mechanical and Industrial Engineering, Faculty of Engineering, Universitas Gadjah Mada, Jl. Grafika No. 2, Yogyakarta, 55281, Indonesia

The authors regret < that Figure 9 in the original published version of this article was incorrect, as it did not represent the intended FTIR

DOI of original article: https://doi.org/10.1016/j.jmrt.2026.04.117.
* Corresponding author.
*E-mail address:* rahmat.doni@mail.unnes.ac.id (R.D. Widodo).

https://doi.org/10.1016/j.jmrt.2026.04.184

Available online 21 April 2026

results. The correct version of Figure 9 is provided below.

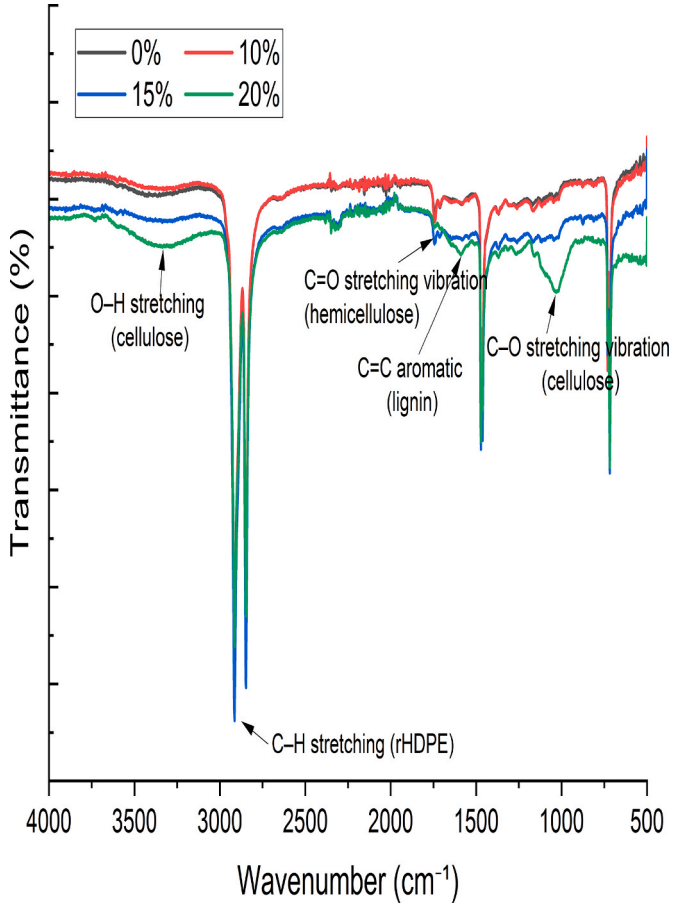


This error does not affect the results or conclusions of the paper. >. The authors would like to apologise for any inconvenience caused.